Formulation of curcumin-loaded solid lipid nanoparticlesproduced by fatty acids coacervation technique

Formulation of curcumin-loaded solid lipid nanoparticles produced by fatty acids coacervation technique.

Daniela Chirio[1], Marina Gallarate[1]*, Elena Peira[1], Luigi Battaglia[1], Loredana Serpe[2], Michele Trotta[1]

[1]*Dipartimento di Scienza e Tecnologia del Farmaco, University of Torino, Italy*

[2]*Dipartimento di Anatomia, Farmacologia e Medicina Legale, University of Torino, Italy*

Abstract

Curcumin (CU)-loaded solid lipid nanoparticles (SLN) of fatty acids (FA) were prepared with a coacervation technique based on FA precipitation from their sodium salt micelles in the presence of polymeric non-ionic surfactants. Myristic, palmitic, stearic, behenic acid, and different polymers with various molecular weights and hydrolysis grades were employed as lipid matrixes and stabilisers, respectively. Generally, spherical shaped nanoparticles with mean diameters below 500 nm were obtained, and only using middle-high hydrolysis grade-polymers SLN with mean diameters lower than 300 nm were produced. CU encapsulation efficiency was in the 28-81% range and was highly influenced by both FA and polymer type. Chitosan hydrochloride was added to FA SLN formulations to produce bioadhesive, positively-charged nanoparticles. A CU-chitosan complex formation could be hypothesised by DSC analysis, UV-VIS spectra and chitosan surface tension determination. A preliminary study on HCT-116 colon cancer cells was developed to evaluate the influence of CU-loaded FA SLNs on cell viability.

Keywords: curcumin, SLN, fatty acids, coacervation

Corresponding author: marina.gallarate@unito.it

phone number: 0039116707081

Introduction

Curcumin (diferuloylmethane) is a yellow pigment derived from the rhizome of the plant *Curcuma Longa* with phenolic groups and conjugated double bounds which is unstable at light and basic pH, degrading within 30 min [1,2].

Although curcumin has shown a wide range of pharmacological activities (chemosensitizing, radiosensitizing, wound healing, antimicrobial, antiviral, antifungal, immunomodulatory, antioxidant and anti-inflammatory) its anticancer properties have attracted a great interest [3]. The anticancer activity of curcumin has been the subject of hundreds of papers and has been reviewed in several recent articles [4,5,6]. Numerous *in vitro* assays using colon cancer cell lines have been performed showing that curcumin possesses anticancer activity, but the underlying mechanisms remain largely to be defined. Moreover, animal model systems have revealed that the diferuloylmethane prevents tumours induced by a diversity of chemical carcinogens in tissues such as skin, breast and liver [7,8]. In the gastrointestinal tract, in particular stomach and duodenum, anticancer properties of curcumin have been also documented [9]. Moreover, epidemiological data suggest that the incidence of several common cancers (i. e., colon, breast, prostate, and lung cancer) is higher in Western countries than in countries such as India, where curcumin is highly consumed [4].

The antitumourigenic property of curcumin has been attributed partly to its ability to inhibit the processes of initiation and promotion in carcinogenesis. Jaiswal et al. [10] demonstrated that curcumin treatment caused p53- and p21-independent G(2)/M phase arrest and apoptosis in human colon cancer HCT-116(p53(+/+)), HCT-116(p53(–/–)) and HCT-116(p21(–/–)) cell lines. A G2/M cell cycle arrest by curcumin was also confirmed in HT-29 human colon cancer cells [11].

Unfortunately, these studies have revealed that curcumin has poor oral bioavailability due to its low water solubility under acidic or neutral conditions. Results from pharmacokinetic assays in animals showed low serum levels of the polyphenol following a single dose administration [12, 13]: about 75% of ingested curcumin was excreted unaltered in the feces and negligible amounts appeared in

the urine. Several human studies have revealed that, after oral administration, the levels of curcumin in plasma are very low (generally in the nanomolar range) while they are higher in colorectal tissue (low micromolar) [14]. This suggests that, outside of the gastrointestinal tract, most of the reported cancer-related effects of curcumin may not be achieved in vivo.

To overcome these bioavailability problems, various methods have been tried to enhance curcumin delivery. Takahashi M. et all [15] prepared liposome-encapsulated curcumin and administered them orally to Sprague-Dawley rats at a dose of 100 mg curcumin/kg body weight. Pharmacokinetic parameters after oral administration of liposomes evidenced higher bioavailability, a faster rate and better absorption of curcumin compared to the other forms. Mukerjee A. et all vehicled curcumin into PLGA nanoparticles and investigated intracellular uptake of curcumin-loaded PLGA nanoparticles in DU145, PC3 and LNCaP cell lines [16]. These nanoparticles were actively taken up by all the cancer cells. Further, to investigate the therapeutic potential of formulation, prostate cancer cell lines, DU145, PC3 and LNCaP were treated with free curcumin, curcumin-loaded PLGA nanoparticles and blank nanoparticles at different concentrations (0-30 μM) for 72 hours and cell proliferation was measured. Curcumin-loaded PLGA nanoparticles exhibited a lower IC50 value in comparison to free curcumin in all cancer cell lines studied. Tønnesen et all [17] prepared complexes between curcumin and cyclodextrin in order to increase the water drug solubility and then its bioavailability. Curcumin had the highest affinity for randomly methylated β-cyclodextrin that increased curcumin solubility at pH 5 of 10^4 factor.

It is well-known that curcumin undergoes rapid hydrolysis under alkaline conditions to yield ferulic acid, its methyl ester and vanillin [18]; it is also very susceptible to photochemical degradation [19]. Curcumin inclusion improves dramatically the hydrolytic stability while decreases its photostability. In a recent study, we [20] vehicled curcumin in solid lipid nanoparticles prepared also with α- and γ-lipophilic cyclodextrins in order to combine advantages of lipid nanoparticles and cyclodextrins. Curcumin fitted better the γ-cyclodextrin cavity, which is larger than that of α-cyclodextrin forming a 2:1 cyclodextrin:curcumin molar ratio complex. A significant reduction in

CU photodegradation was noted when the drug was vehicled in tristearin-SLN, which became less pronounced in the presence of CD-derivatives. The hydrolytic stability of curcumin was highly improved by drug loading in tristearin-SLN and this seemed not to be influenced by the presence of CD derivatives. The presence of cyclodextrins into nanoparticles improved up to 20 folds the curcumin skin uptake compared to drug solution and up to 3 folds compared to nanoparticles in the absence of cyclodextrins.

In the present work a new, solvent-free technique was used to produce curcumin-loaded SLN of fatty acids by acidification of a micellar solution of their alkaline salts [21]. The use of myristic, palmitic, stearic and behenic acids as lipid matrices and of different non-ionic polymeric surfactants as stabilisers was investigated. The aim was to individuate the best lipid and stabiliser composition to optimise SLN mean diameters and curcumin entrapment efficiency. After characterising SLN by determining their physico-chemical properties, a preliminary *in vitro* study was developed to test SLN in HCT116 human colon adenocarcinoma cells to evaluate the influence of curcumin-loaded SLN on cell viability.

Methods

Materials

Citric acid, phosphoric acid, lactic acid, sodium phosphate dibasic and sodium phosphate monobasic were purchased from A.C.E.F. (Fiorenzuola d'Arda, Italy), 98% hydrolysed PVA 14000–21000 Mw (PVA 14000) from BDH Chemicals (Poole, UK); 80% hydrolysed PVA 9000–10000 Mw (PVA 9000), 89% hydrolysed PVA 85000–124000 Mw (PVA 85000), sodium myristate (Na-M), curcumin (CU), Pluronic F127 (PLF127), Pluronic F68 (PLF68), dextran and trehalose from Sigma (Dorset, UK); Poval PVA L10, Poval PVA L508, L polymer L9-78 and LM polymer LM20 from Kuraray (Kurashiki City, Japan), sodium stearate (Na-S), sodium palmitate (Na-P), myristic acid (MA), palmitic acid (PA), behenic acid (BA), polyvinylpyrrolidone K15 (Mw 10,000 - PVP 10,000) and polyvinylpyrrolidone K25 (Mw 24,000 – PVP 24,000) from Fluka (Buchs,

Switzerland); HPMC 2910 (hydroxypropylmethyl cellulose, 28–30% methyl substitution degree, 7–12% isopropyl substitution degree) and 15cP (Benecel E15—14000 Mw), 50cP (Benecel E50—21000 Mw) were purchased from Eigenmann & Veronelli (Rho, Italy); stearic acid (SA) and Arabic gum from Merck (Darmstadt, Germany); polyvinylpyrrolidone K12 (Mw 3500 – PVP 3500) from Acros Organics (Geel, Belgium). Sodium behenate (Na-B) was obtained by adding a stoichiometric amount of NaOH ethanolic solution to the ethanolic solution of BA: the soap was purified by re-crystallisation and stored in an essicator at room temperature. 22% hydrolysed dextran (DexP) was obtained by adding 10 ml 0.1 M NaOH and 200 µl 2,3 epoxypropyl-phenylether to 1g dextran: the mixture was stirred up to have clear solution. Deionised water was obtained by a MilliQ system (Millipore, Bedford, MO). All other chemicals were analytical grade and used without any further purification.

SLN preparation

SLN were prepared by the coacervation method [21]. Different operative conditions were used for SLN preparation according to the fatty acids (FA) under study. Stock solutions of each polymeric stabiliser (PVA 9000, PVA 14000, PVA 85000, PVA L508, PVA L10, PVA LM20, PVA L9-78, PL F68, PL F127, DexP, chitosan hydrochloride, PVP 3500, PVP 10000, PVP 24000, arabic gum) at appropriate concentrations were prepared by heating the polymer in water and then cooling at room temperature. Briefly, 1% w/w each FA sodium salt was dispersed in each polymeric stabiliser stock solution and the mixture was then heated under stirring (300 rpm) just above the Krafft point of FA sodium salt to obtain a clear solution. A fixed amount of 8.3 mg/ml ethanol CU solution was added to the warm aqueous Na-FA solution just above the Krafft point of FA sodium salt at a final concentration of 6% v/v. A selected acidifying solution (coacervating solution) was then added drop-wise until pH 4.0 was reached (Table 1). The obtained suspension was then cooled in a water bath under stirring at 300 rpm until 15°C temperature was reached.

SLN characterisation

The morphology of SLN and curcumin localisation were determined using optical microscopy equipped with a fluorescent lamp (Leica DM 2500, Germany).

SLN particle sizes and polydispersity indexes were determined using laser light scattering technique—LLS (Brookhaven, USA). Measurements were obtained at an angle of 90°. The dispersions were diluted with water for size determination or with 0.01 M KCl for Zeta-potential determination, in order to achieve the prescribed conductibility.

DSC analysis were performed with a DSC 7 Perkin-Elmer differential calorimeter (Norwalk, CT, USA). Lipid bulk material and SLN suspensions were placed into conventional aluminium pans and heated from 30° to 70°C at 2°C min^{-1}. The degree of crystallinity of SLN was estimated by calculating the ratio between the melting enthalpy/g lipid in SLN dispersion and the melting enthalpy/g of the bulk material [22,23].

CU entrapment efficiency (EE%) was calculated as the ratio between CU amount in SLN and that in the starting micellar solution × 100. CU analysis was performed as follows: 1 ml SLN suspension was centrifuged for 30 min at 24,000 rpm, the precipitate was washed twice with 1 ml ethanol/water 20/80 to eliminate adsorbed CU. The solid residue was dissolved in 1 ml ethanol, 2 ml water were then added to precipitate the lipid matrix and the supernatant obtained was injected in HPLC for CU quantification. HPLC analysis was performed using a LC9 pump (Shimadzu, Japan) with an Allsphere ODS-2 5 μ 150×4.6mm column and a C-R5A integrator (Shimadzu, Japan); mobile phase: $CH_3OH/H_2O/CH_3COOH$ 70/30/1 (flow rate 1ml min^{-1}); detector: UV λ=450 nm (Shimadzu, Japan). Retention time was 5.5 min.

The limit of quantification (LOQ), defined as the lowest curcumin concentration in the curve that can be measured routinely with acceptable precision and accuracy, was 0.7 μmol/ml; the limit of determination (LOD), defined as the lowest detection limit, was 0.3 μmol/ml (signal to noise>2.0).

Chitosan surface tension determination

All measurements were performed at 25.0±0.1 °C using a ring tensiometer (Krüss, K10, Germany). Surface tension measurements were executed on chitosan water solution and on chitosan 1% w/w PVA 9000 aqueous solution. Briefly, 6 mg/ml chitosan water solution and 6 mg/ml chitosan 1%w/w PVA 9000 aqueous solution were prepared and utilised as starting solution. Each solution was then diluted with water or 1% PVA 9000 aqueous solution in order to determine chitosan surface tension in the 0.5-6 mg/ml concentration range. pH of each solution was 5.0.

CU-chitosan complex characterisation

To verify the formation of CU-chitosan complex CU UV-VIS absorption spectra in the presence of different chitosan concentration were carried out.

Briefly, 3.75, 5, 7.5, 10, 15 mg chitosan were dissolved in 9.9 ml water brought to pH 4. 100 µl 3 mg/ml CU ethanol solution were added to each sample. Suspensions were stirred for 4 h and then centrifuged 10 min at 25000 rpm. A spectrum of the supernatant was registered by UV-VIS spectrophotometer from 200 to 600 nm.

SLN and CU stability

Sizes and CU EE% of PA-SLN stabilised with PVA 9000 or PVA L508 or chitosan + PVA 9000 were monitored for 3 months to study SLN physical stability and CU chemical stability. Mean sizes were determined by LLS and CU EE% overtime was obtained by HPLC.

Same SLN suspensions were freeze-dried without adding any cryoprotectant (FD-SLN) and in the presence of 2% w/v threalose (FD-THR-SLN) by using a Modulyo Freeze Dryer (Edwards Alto Vuoto, Italy). The resulting samples were characterised by LLS analysis.

Preliminary *in vitro* cytotoxicity studies

In vitro cytotoxicity studies were set up with HCT-116 colon cancer cells. Approximately 2500 cells were seeded in 96-well plates and were allowed to attach and proliferate for a period of 24 h. The cells were then incubated with various dosages of different SLN types. Cell cytotoxicity was determined after incubation of 24 and 48 h. SLN were removed and the cells were treated with 1:10

diluted WST-1 medium (Roche, Italy). Plates were incubated 2 h at 37°C to form crystals of formazan by the metabolically active cells. Finally, plates were read spectrophotometrically at 450 nm. Cell viability was calculated as a percentage of the control. All experiments were carried out three times, each condition being performed eightfold.

Samples under study:

SLN: MA-PVA L508, P.A.-PVA L508 and S.A.-PVA L508 1:50 diluted (CU= $2.7 \cdot 10^{-5}$M, MA= $8.8 \cdot 10^{-4}$M, PA=$7.8 \cdot 10^{-4}$M, SA=$7.0 \cdot 10^{-4}$M); S.A.-PVA L508, S.A.-PVA L508-CU, S.A.-PVA 9000, S.A.-PVA 9000-CU, 1:100 (CU= $1.4 \cdot 10^{-5}$M, SA= $3.5 \cdot 10^{-4}$M), 1:200 (CU= $6.8 \cdot 10^{-6}$M, SA= $1.7 \cdot 10^{-4}$M), 1:1000 (CU= $1.4 \cdot 10^{-6}$M, SA= $3.5 \cdot 10^{-5}$M) diluted.

Suspensions: CU-PVA L508, CU-PVA 9000 1:100 (CU= $1.4 \cdot 10^{-5}$M), 1:200 (CU= $6.8 \cdot 10^{-6}$M), 1:1000 (CU= $1.4 \cdot 10^{-6}$M) diluted.

Statistical analysis

Statistical analysis of differences between varying SLN samples and the control was performed using one-way analysis of variance (one-way ANOVA). A 0.05 level of probability was taken as the minimal level of significance.

Results

SLN characterisation

By FA coacervation method CU-loaded SLN were obtained with all FA tested. Several polymeric stabilisers at different molecular weight and various hydrolysis grade were used. Both FA and stabilisers were used at 1% w/w, just as in previous works. In Table 2 mean diameters and polydispersion indexes of SLN prepared with different FA and stabilisers are reported. As it can be noted, several SLN had diameters below 500 nm; particularly, using PVA polymers with middle-high hydrolysis grade (PVA 9000, PVA L508, PVA L-10) SLN with size lower than 300 nm were

obtained. PVA type seems therefore to influence SLN mean diameters and polydispersity, probably due to different interactions between the lipid matrix and the stabiliser, that might depend both on hydrolysis degree and polymer molecular weight. The influence of PVA type on size is also described in literature: Hong et al. reported that in PVA-stabilised emulsions, low hydrolysis degree-polymers determine a reduction of emulsion droplet sizes.

Also FA type seemed to affect SLN sizes: the smallest CU-loaded SLN (mean diameter lower than 200 nm) were obtained using PA, as also reported in a previous work [21]. The differences in mean sizes among different FA-SLN can probably be related to a number of factors, such as the operating temperature, FA chain length and stabilisers concentration, which varied in the production process of the different FA-SLN.

Other polymeric stabilisers were used as an alternative to PVA: PLF produced SLN in the 400-1300 nm range, PVP in the 300-4600 nm range, different viscosity-HPMC in the 400-5000 nm range. Enhancing the viscosity of the medium, as in HPMC samples, an increase in the mean size of resultant nanoparticles was noted; also in literature it is reported that an increase of aqueous medium viscosity may cause an increase of SLN particle size [24].

Using DexP as stabilizer, SLN in the 290-500 nm range were obtained. Chitosan hydrochloride was added to FA-PVA 9000 SLN formulations to produce bioadhesive, positively-charged nanoparticles. Using MA and SA as matrix, SLN of about 350-400 nm were obtained.

The observation of SLN nanosuspension under microscope light confirmed both the spherical shape of the particles and the dimensional range. The use of fluorescent light allowed to locate CU in SLN nanosuspensions: homogeneous dispersions of fluorescent nanoparticles were observed with middle-high hydrolysis degree PVA, non-loaded CU yellow crystals were detectable in other formulations (data not shown).

In Table 3 Zeta potential values are reported. Almost all formulations showed slight negative charge with values in the -2.7 : -6.0 range. Probably charges are due to carboxyl groups of FA sodium salts, present in traces on the particles surface. On the contrary, positive charges are shown by chitosan

nanoparticles; indeed, at final pH of SLN suspension, chitosan is positively-charged and can interact with carboxyl groups on nanoparticles surface conferring them a positive charge.

In Table 4 CU EE % in small-sized SLN prepared with different FA is reported. As it can be noticed, EE % was in the 28-81% range and was highly influenced by both FA and polymer type; probably CU EE % depends on both the preparation methods used for various FA and the solubilising properties of stabilisers, which could auto-assembly in the aqueous medium modifying CU solubility in the dispersing medium. Generally, the highest CU EE % was scored in PA-SLN; among the studied stabilisers, the highest CU EE% was observed in the presence of PVA 9000, which had the lowest efficiency in improving CU water solubility.

The solid state of SLN after coacervation was verified by differential scanning calorimetry. DSC thermograms of PA and SA SLN in the presence and in the absence of CU were depicted in Figure 1-4. In Figure 1 PA SLN thermograms in the absence of CU are reported.

As already noted in a previous work [21], DSC thermograms of SLN showed only small differences between the melting point of raw lipid and that of the corresponding SLN. According to Siekmann and Westesen [23], the melting point decrease of SLN colloidal systems can be due to the colloidal dimensions of the particles, in particular to their high surface-to-volume ratio, and not to the re-crystallisation of the lipid matrices in a metastable polymorph. The presence of impurities, surfactants and stabilisers could also affect this phenomenon [25, 26]. An evident decrease of enthalpy respect raw FA (from 201 J/g to 77 J/g) was noted in the PA-PVA 9000-chitosan SLN thermogram. This result could indicate a different interaction between lipid and chitosan; probably, as supposed from Zeta potential measurements, the polymer might interact with carboxyl groups of the lipid present on particles surface.

In Figure 2 SA SLN thermograms in the absence of CU are reported. In this case a significant SLN transition temperature decrease compared to raw SA was noted. This difference can be ascribed to polymorphism. In fact SA can exist in 3 crystalline forms, A-B-C [27], with 3 different melting points (43°**C,** 54°C, 69°C respectively). Previous investigation on SA-SLN with X-rays [21]

confirmed that, in SLN, SA was in the low melting B form, which is characterised by monoclinic lattice [28].

SA polymorphism is typical of coacervation process regardless the presence of a stabiliser [21]. B form of SA was also obtained after acidification of Na-S solution with lactic acid in the absence of PVA.

Also in this case chitosan-SLN present the lowest transition enthalpy, indicating a stronger lipid-polymer interaction.

In Figures 3 and 4 DSC thermograms of CU-loaded SLN are reported. In PA-PVA 9000 and PA-PVA L508 SLN the presence of CU influences neither temperature nor transition enthalpy. A different behaviour can be observed in PA-PVA 9000-chitosan SLN: the transition peak was 3°C shifted to higher temperatures and the transition enthalpy was halved. These results might probably be due to different CU localisation, as in PVA 9000 and PVA L508 SLNs it could be uniformly dispersed throughout the lipid matrix, while in PVA 9000-chitosan SLNs it could be more concentrated on the outer surface. In all SA SLN formulation a significant influence of CU on transition peak was noted: with PVA 9000 and PVA L508 in the presence of CU a marked temperature drop was noted, while with PVA 9000-chitosan an enthalpy transition decrease was also observed. Probably in SA-SLN CU is mostly located on the surface when compared with PA SLNs, minimising the effect due to the presence of chitosan on the surface.

From these observations, a CU-chitosan complex formation could therefore be hypothesised, which was further investigated by CU UV-VIS absorption studies in the presence of different chitosan concentrations and by chitosan surface tension determination.

UV-VIS absorption spectra of 30 μg/ml ($8.14 \cdot 10^{-5}$ M) CU aqueous solutions showed a progressive increase of CU absorbance at 420 nm as a function of chitosan concentration (Figure 5). 1:12 to 1:50 CU:chitosan w/w ratio were examined. The marked increase in CU aqueous solubility was not ascribable to a possible micellisation in chitosan micelles, as evidenced by surface tension measurements. Indeed, a chitosan critical association concentration (CAC) was evidenced both in

water and in PVA 9000 aqueous solution at pH 5.0 (Figure 6-7). Chitosan CACs were quite higher than those used in solubility studies and in SLN preparation process.

The lower CU EE% observed in chitosan-stabilised SLN could therefore be ascribed to an enhanced CU water solubility, due to the formation of a hydrophilic complex with chitosan. As CU water solubility is generally considered one of the most important hurdle to CU administration, the possibility of using a hydrophilic complex could represent a preamble to further development of CU dosage forms, even if it may be undesirable in SLN production.

SLN and CU stability

In order to evaluate the stability of CU-loaded SLN suspensions, LLS measurements and EE% determinations were performed for 12 weeks. In Table 5 SLN sizes are reported; all analysed formulations were stable for 12 weeks, as only very low increases in SLN sizes were noted.

In Table 6 CU EE% over time are shown. After 12 weeks, a 15% CU loss was noted in all samples; a 6.5% and 13.6% decrease of CU EE% was noted in PA-PVA 9000 and PA-PVA L508 SLN respectively, while a mild increase of non-loaded CU and adsorbed CU was observed. These results can suggest that CU was slowly released from SLN, partially solubilised in polymeric stabilisers solution and partially adsorbed onto nanoparticle surface. At the same time, a more evident CU EE% decrease and adsorbed-CU increase were observed in PA-PVA9000-chitosan SLN, confirming the formation of a CU-chitosan complex, that, mainly located on SLN surface, contributes to enhance the amount of adsorbed CU. Moreover, the presence of chitosan in the bulk PVA solution could further improve CU aqueous solubilisation.

To verify the possibility of decreasing both CU degradation and CU release from SLN occurring in an aqueous medium, PA-PVA 9000, PA-PVA L508 and PA-PVA 9000-chitosan SLN-suspensions were freeze-dried in the absence of cryoprotectants (FD-SLN) and in the presence of 2% w/v threalose (FD-THR-SLN). SLN mean diameters and polydispersities before and after freeze-drying are reported in Table 7. Similar values in mean diameters after freeze-drying were obtained without

any cryoprotectant only for PA-PVA9000 SLN; mean diameters of PA-PVA 9000 and PA-PVA9000-chitosan SLNs could be maintained only in the presence of threalose.

***In vitro* cytotoxicity studies**

The preliminary study on HCT-116 colon cancer cells was developed to evaluate the influence of CU-loaded SA SLN on cell viability. Among different FA SLN prepared, SA SLN were chosen for cell survival studies, as, in preliminary text, SA revealed the lowest citotoxicity on HCT-116 colon cancer cell compared with MA and PA; BA was not texted, as BA SLN did not present physico-chemical characteristics suitable to CU entrapment.

Figures 8 and 9 show the survival histograms of HCT-116 after 24 and 48 h exposure to the different CU-loaded and unloaded SLN at various dilution. CU aqueous PVA 9000 and PVA L508 suspensions were chosen as blanks.

After 24 h incubation, at the highest CU concentration (1:100 dilution), both CU suspensions showed citotoxicity, as a decrease of cell growth of 35% (PVA 9000) and of 30% (PVA L508) was noted: this effect was quite dampened at the lowest CU concentrations (1:200, 1:1000 dilutions) with a residual cell survival of almost 80%. At 1:100 and 1:200 dilution, no significant difference was noted between CU-loaded and unloaded SLN, probably being the citotoxicity of SLN not negligible. At 1:1000 dilution a flattening of the survival histogram occurred, probably as CU concentration was too low to exert an effect by itself.

At 48 h, at each dilution, CU PVA 9000 suspension loosed its citotoxicity, probably owing to its the very low CU solvent efficiency, which probably allowed a renewed cell viability: this effect was not noted for CU PVA L508 suspension, having PVA L508 a better CU solvent efficiency. Citotoxicity of each CU-loaded and unloaded SLN were quite similar, more pronounced at 1:200 and 1:100 than at 1:1000 dilution.

These rather unsuccessfully results indicate the necessity to develop CU colloidal carriers able to entrap higher CU amounts, in order to treat cell cultures with higher CU concentrations in the presence of lipid matrices showing a as low as possible citoxicity.

Conclusions

The use of FA coacervation technique permitted to obtain CU-FA SLN with sizes below 300 nm and with EE% in the 28-81% range, depending on FA and polymer type employed; the formulation study showed more suitable the employ of middle-high hydrolysis grade-polymers. The introduction of chitosan hydrocloride in FA formulation produced bioadhesive, positively-charged nanoparticles and evidenced a water-soluble CU-chitosan complex probable formation, as confirmed by DSC analysis, UV-VIS spectra and chitosan surface tension.

SLN-suspensions sizes were stable until 12 weeks while CU delivery decreased until 85% in the same time; the freeze-drying process in the presence or in the absence of cryoprotectant could enhance the CU stability. The preliminary study on HCT-116 colon cancer cells evidenced the necessity to develop CU colloidal carriers able to entrap higher CU amounts, in order to treat cell cultures with higher CU concentrations in the presence of lipid matrices showing an as low as possible citoxicity.

Acknowledgment

The research was supported by a grant of the Italian Minister of Research (MIUR) under PRIN 06 program

References

1 Tonnesen HH, Karlsen J, Van Henegouwen GB. Studies on curcumin and curcuminoids: VIII – photochemical stability of curcumin, Z. Lebensm. Unters. Forsch, 1986; 183:116–122.

2 Wang YJ, Pan MH, Cheng AL, Lin LI et al. Stability of curcumin in buffer solutions and characterization of its degradation products. J. Pharm. Biomed. Anal, 1997; 15:1867–1876.

3 Villegas I, Sánchez-Fidalgo S, Alarcón de la Lastra C. New mechanisms and therapeutic potential of curcumin for colorectal cancer. Mol. Nutr. Food Res., 2008; 52:1040 – 1061.

4 Aggarwal BB, Kumar A, Bharti AC. Anticancer potential of curcumin: Preclinical and clinical studies. Anticancer Res., 2003; 23:363 –398.

5 Chauhan DP. Chemotherapeutic potential of curcumin for colorectal cancer. Curr. Pharm. Des., 2002; 8:1695–1706.

6 Thangapazham RL, Sharma A, Maheshwari RK. Multiple molecular targets in cancer chemoprevention by curcumin. AAPS J, 2006; 8:E443–E449.

7 Huang MT, Lysz T, Ferraro T, Abidi TF et al. Inhibitory effects of curcumin on in vitro lipoxygenase and cyclooxygenase activities in mouse epidermis. Cancer Res., 1991; 51:813–819.

8 Lopez-Lazaro M, Willmore E, Jobson A, Gilroy KL et al. Curcumin induces high levels of topoisomerase I- and II-DNA complexes in K562 leukemia cells. J. Nat. Prod., 2007; 70:1884 – 1888.

9 Strick R, Strissel PL, Borgers S, Smith SL, Rowley JD. Dietary bioflavonoids induce cleavage in the MLL gene and may contribute to infant leukemia. Proc. Natl. Acad. Sci. USA 2000; 97:4790–4795

10 Jaiswal AS, Marlow BP, Gupta N, Narayan S. Betacatenin-mediated transactivation and cell-cell adhesion pathways are important in curcumin (diferuylmethane)-induced growth arrest and apoptosis in colon cancer cells. Oncogene, 2002; 21:8414 –8427.

11 Van Erk MJ., Teuling E, Staal YC, Huybers S et al. Time- and dose-dependent effects of curcumin on gene expression in human colon cancer cells. J. Carcinog., 2004; 3:8–17.

12 Cheng AL, Hsu CH, Lin JK, Hsu MM et al. Phase I clinical trial of curcumin, a chemopreventive agent, in patients with high-risk or pre-malignant lesions. Anticancer Res., 2001; 21:2895 –2900.

13 Sharma RA, McLelland HR, Hill KA, Ireson CR et al. Pharmacodynamic and pharmacokinetic study of oral Curcuma extract in patients with colorectal cancer. Clin. Cancer Res., 2001; 7:894–1900

14 López-Lázaro M. Anticancer and carcinogenic properties of curcumin: Considerations for its clinical development as a cancer chemopreventive and chemotherapeutic agent. Mol. Nutr. Food Res., 2008; 52:103 –S127

15 Takahashi M, Uechi S, Takara K, Asikin Y, Wada K. Evaluation of an oral carrier system in rats: bioavailability and antioxidant properties of liposome-encapsulated curcumin. J Agric Food Chem., 2009; 14; 57: 9141-6.

16 Mukerjee A, Vishwanatha JK. Formulation, characterization and evaluation of curcumin-loaded PLGA nanospheres for cancer therapy. Anticancer Res., 2009; 29: 3867-75.

17 Tønnesen HH, Másson M, Loftsson T. Studies of curcumin and curcuminoids. Cyclodextrin complexation: solubility, chemical and photochemical stability. Int. J. Pharm, 2002; 244:127-135.

18 Lin JK, Pan MH, Shiau SYL. Recent studies on the biofunctions and biotransformations of curcumin. Biofactors, 2000; 13:53-158.

19 Pfeiffer E, Hohle S, Solyom A, Metzler M. Studies on the stability of turmeric constituents. J. Food Eng., 2003; 56:257-259.

20 Chirio D, Gallarate M, Trotta M, Carlotti ME, Calcio Gaudino E, Cravotto G. Influence of α- and γ- cyclodextrin lipophilic derivatives on curcumin-loaded SLN. J. Incl. Phenom. Macrocycl. Chem., 2009; 65:391–402.

21 Battaglia L, Gallarate M, Cavalli R, Trotta M. Solid lipid nanoparticles produced through a coacervation method. J. Microencapsulation, 2010; 27: 78–85.

22 Siekmann B, Westesen K. Thermoanalysis of the recrystallization process of melt-homogenized glyceride nanoparticles. Colloid Surf. B., 1994; 3:159–175.

23 Freitas C, Müller RH. Correlation between longterm stability of solid lipid nanoparticles (SLN) and crystallinity of the lipid phase. Eur. J. Pharm. Biopharm., 1999; 47:125–132.

24 Schubert MA, Müller-Goymann CC. Solvent injection as a new approach for manufacturing lipid nanoparticles—evaluation of the method and process parameters. Eur. J. Pharm. Biopharm., 2003; 55:125–131

25 Hou D, Xie C, Huang K, Zhu C. The production and characteristics of solid lipid nanoparticles (SLN). Biomaterials, 2003; 24:1781–1785.

26 Liu J, Gong T, Wang C, Zhong Z, Zhang Z. Solid lipid nanoparticles loaded with insulin by sodium cholate-phosphatidylcholine-based mixed micelles. Preparation and characterisation. Int. J. Pharm., 2007; 340:153–162.

27 Raghavan R, Burchett M, Loffredo D, Mulligan JA. Low-Level (PPB) Determination of cisplatin in cleaning validation (Rinse Water) samples. II. A High-Performance Liquid Chromatographic Method. Drug Develop. Ind. Pharmacy. 2000; 6:429-440.

28 Goto M, Asada E. The crystal structure of the B-form of stearic acid. Bull. Chem. Soc. Jap., 1978; 51:2456–2459.

Sodium salt	Coacervating solution
Na-M	1M Na_2HPO_4 + 1M citric acid
Na-P	1M citric acid
Na-S	1M lactic acid
Na-B	1M NaH_2PO_4 and then1M HCl

Table 1 Coacervating solutions for each FA sodium salt

	SIZES (nm) POLYDISPERSION INDEX			
	MA-SLN	PA-SLN	SA-SLN	BA-SLN
PVA 9000 50 mg -	261.6 ± 14.5 0.134	193.3 ± 2.7 0.087	345.0 ± 16.3 0.167	299.2 ± 0.3 0.055
PVA 9000 50 mg - CHIT. HCl. 7.5 mg	369.1 ± 14.8 0.166	781.0 ± 19.3 0.144	402.8 ± 21.5 0.125	1141 ± 51 0.091
PVA 14000 50 mg	2753 ± 337 0.370	2168 ± 1161 0.301	3364 ± 82 0,553	1027 ± 106 0.268
PVA 85000-124000 50 mg	375.6 ± 19.2 0.089	573.8 ± 13.3 0.223	723.7 ± 67.6 0.329	415.1 ± 8.1 0.184
PVA 85000-146000 50 mg	295.2 ± 24.8 0.090	422.4 ± 0.4 0.159	626.8 ± 31.4 0.339	964.6 ± 69.0 0.245
PVA L10 50 mg	289.9 ± 3.4 0.178	188.5 ± 0.8 0.194	299.4 ± 6.2 0.142	335.9 ± 9.3 0.228
PVA L508 50 mg	255.3 ± 6.4 0.110	182.2 ± 6.2 0.234	317.9 ± 17.2 0.177	307.1 ± 4.5 0.240
PVA L9-78 50 mg	327.5 ± 5.6 0.059	222.6 ± 2.5 0.152	302.1 ± 8.6 0.208	329.7 ± 4.0 0.120
PVA LM20 50 mg	> 5000 > 0.500	> 5000 > 0.500	> 5000 >0.500	> 5000 > 0.500
PLF68 50 mg	403.7 ± 40.0 0.208	1372 ± 186 0.332	529.3 ± 13.9 0.332	411.8 ± 221.9 0.420
PLF127 50 mg	736.7 ± 42.6 0.367	651.7 ± 29.0 0.087	478.2 ± 44.4 0.345	297.7 ± 37.9 0.239
DEXP 22% 15 mg	322.3 ± 22.1 0.092	405.6 ± 32.7 0.281	290.8 ± 2.5 0.063	290.8 ± 2.5 0.063
HPMC E15 50 mg	1416 ± 141 0.364	> 5000 > 0.500	635.5 ± 76.1 0.269	> 5000 > 0.500
HPMC E50 50 mg	> 5000 > 0.500	> 5000 > 0.500	630.7 ± 48.0 0.270	> 5000 > 0.500
PVP 3500 50 mg	2473 ± 281 0.239	4618.0 ± 419.8 0.415	4497 ± 869 0.096	> 5000 > 0.500
PVP 10000 50 mg	1236 ± 134 0.106	1851 ± 213 0.248	2795 ± 553 0.499	2893 ± 333 0.193
PVP 24000 50 mg	396.1±25.8 0.214	388.2 ± 38.0 0.258	263.5 ± 3.2 0.098	1222 ± 201 0.371

Table 2 CU-loaded FA-SLN sizes and polydispersion indexes (PI). Formulations were referred to 50 mg FA and 2.5 mg CU into 5 ml suspension.

SLN	ZETA POTENTIAL (mV)
PA 50 mg - PVA 9000 50 mg	- 6.05 ± 1.07
PA 50 mg- PVA 9000 50 mg - CHIT. HCl 7.5 mg	+ 3.41 ± 0.60
PA 50 mg - PVA L10 50 mg	- 2.73 ± 0.79
PA 50 mg - PVA L508 50 mg	- 4.32 ± 0.56
PA 50 mg - PVA L9-78 50 mg	- 3.04 ± 0.56
PA 50 mg - PVA 9000 50 mg - CU 2.5 mg	- 3.90 ± 0.80
PA 50 mg- PVA 9000 50 mg-CHIT. HCl. 7.5 mg-CU 2.5 mg	+ 22.13 ± 3.19
PA 50 mg - PVA L10 50 mg - CU 2.5 mg	- 4.35 ± 0.83
PA 50 mg - PVA L508 50 mg - CU 2.5 mg	- 3.30 ± 0.47
PA 50 mg - PVA L9-78 50 mg - CU 2.5 mg	- 3.34 ± 0.79

Table 3 Zeta potential values of PA nanoparticles.

	CU EE% FREE CU % ADSORBED CU%			
	MA-SLN	PA-SLN	SA-SLN	BA-SLN
PVA 9000 50 mg -	48.4 25.4 26.2	81.4 10.2 8.4	64.6 29.0 6.4	28.8 61.6 9.6
PVA 9000 50 mg - CHIT. HCl. 7.5 mg	49.9 36.0 14.1	60.7 28.1 11.2	45.4 47.4 7.2	-
PVA 85000-124000 50 mg	39.6 45.9 14.5	-	-	33.5 62.4 4.1
PVA L10 50 mg	40.3 36.1 23.6	62.2 19.9 17.9	43.5 51.2 5.3	28.9 64.4 6.7
PVA L508 50 mg	42.3 37.0 20.7	65.6 23.2 11.2	35.4 60.1 4.5	51.9 32.6 15.5
PVA L9-78 50 mg	54.5 36.0 9.5	64.1 20.1 15.8	43.5 36.6 19.9	66.3 28.6 5.1
PLF127 50 mg	-	-	-	28.2 66.7 5.1
DEXP 22% 15 mg	59.9 0.2 39.9	-	43.8 0.2 56.0	
PVP 24000 50 mg	35.4 49.8 14.8	35.4 49.7 14.9	38.6 52.6 8.8	

Table 4 CU EE% of FA SLN. Formulations were referred to 50 mg FA and 2.5 mg CU into 5 ml suspension.

	PA-PVA 9000	PA-PVA L508	PA-PVA9000-CHITOSAN
T_o	253.4 ± 5.5 (0.033)	182.5 ± 3.9 (0.230)	344.2 ± 20.9 (0.210)
2 weeks	245.1 ± 13.3 (0.142)	212.1 ± 4.3 (0.252)	343.4 ± 27.7 (0.242)
4 weeks	242.1 ± 16.9 (0.109)	220.9 ± 2.4 (0.233)	355.2 ± 22.2 (0.222)
8 weeks	272.5 ± 4.0 (0.133)	244.4 ± 6.8 (0.271)	381.1 ± 11.6 (0.226)
12 weeks	275.9 ± 1.9 (0.159)	246.8 ± 9.4 (0.277)	391.5 ± 15.8 (0.213)

Table 5 PA SLN sizes (nm) and PI determined over 12 weeks.

	PVA 9000		PVAL508		PVA9000-CHIT HCl	
	CU AMOUNT (%)	CU EE% FREE CU% ADSORBED CU%	CU AMOUNT (%)	CU EE% FREE CU% ADSORBED CU%	CU AMOUNT (%)	CU EE% FREE CU% ADSORBED CU%
T_0	100	81.0 11.6 7.4	100	65.6 18.9 15.5	100	60.7 28.1 11.2
4 weeks	92.7	76.4 13.8 9.8	94.8	60.9 20.6 18.5	98.2	56.4 9.7 33.9
8 weeks	86.1	74.8 14.9 10.3	87.2	54.9 21.4 23.7	95.5	56.9 6.9 36.2
12 weeks	85.0	74.4 15.0 10.6	85.4	52.0 23.0 25.0	88.3	43.3 4.9 51.8

Table 6 CU EE% of PA SLN determined over 12 weeks. Formulations were referred to 50 mg PA, 50 mg stabiliser and 2.5 mg CU into 5 ml suspension.

	PA-PVA 9000 (nm)	PA-PVA L508 (nm)	PA-CHIT HCl (nm)
T_o	253.4 ± 5.5 (0.033)	182.5 ± 3.9 (0.230)	344.2 ± 20.9 (0.210)
after freeze-drying without any crioprotectant	288.6 ± 17.0 (0.207)	616.1 ± 71.5 (0.334)	523.4 ± 50.3 (0.282)
after freeze-drying with 2% w/v threalose	275.3 ± 10.7 (0.184)	206.6 ± 8.0 (0.223)	402.5 ± 41.8 (0.210)

Table 7 PA SLN sizes (nm) and PI determined after freeze-drying in the presence and in the absence of cryoprotectant.

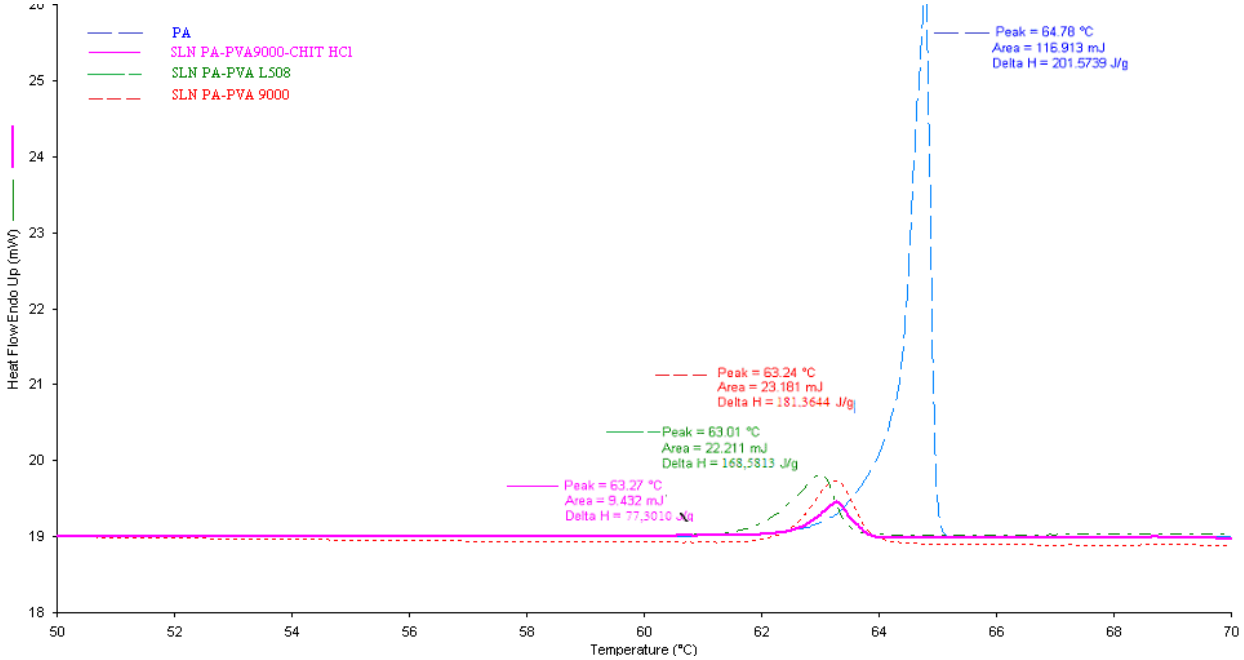

Figure 1 DSC thermograms of PA SLN in the absence of CU

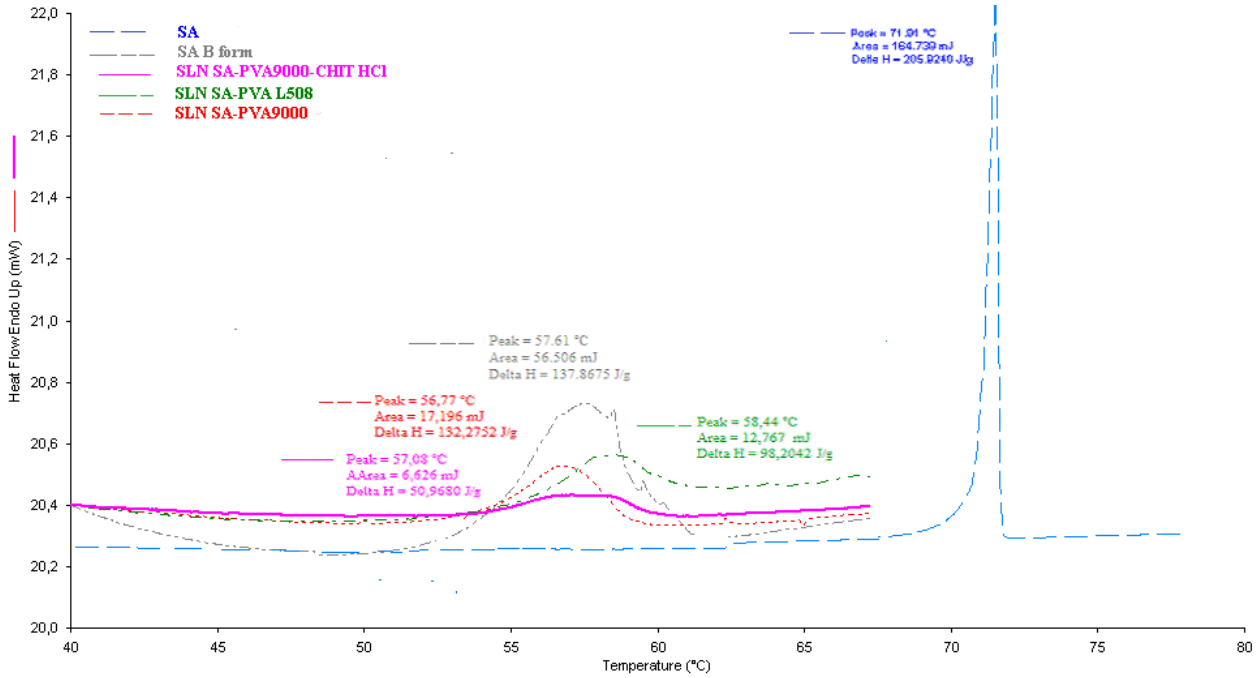

Figure 2 DSC thermograms of SA SLN in the absence of CU.

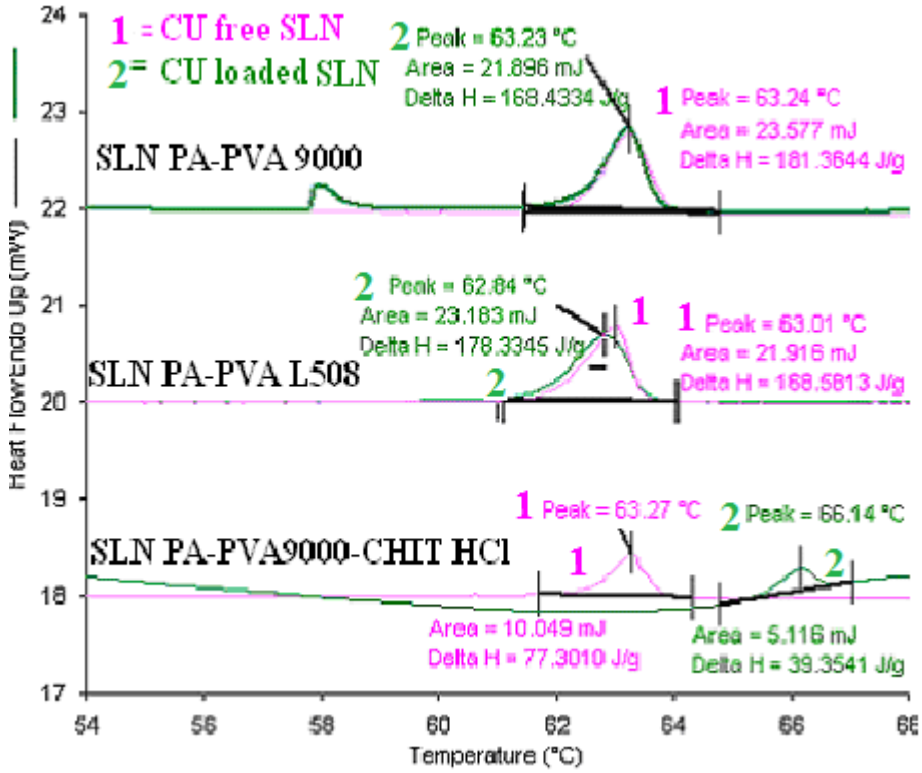

Figure 3 DSC thermograms of PA SLN in the presence and in the absence of CU.

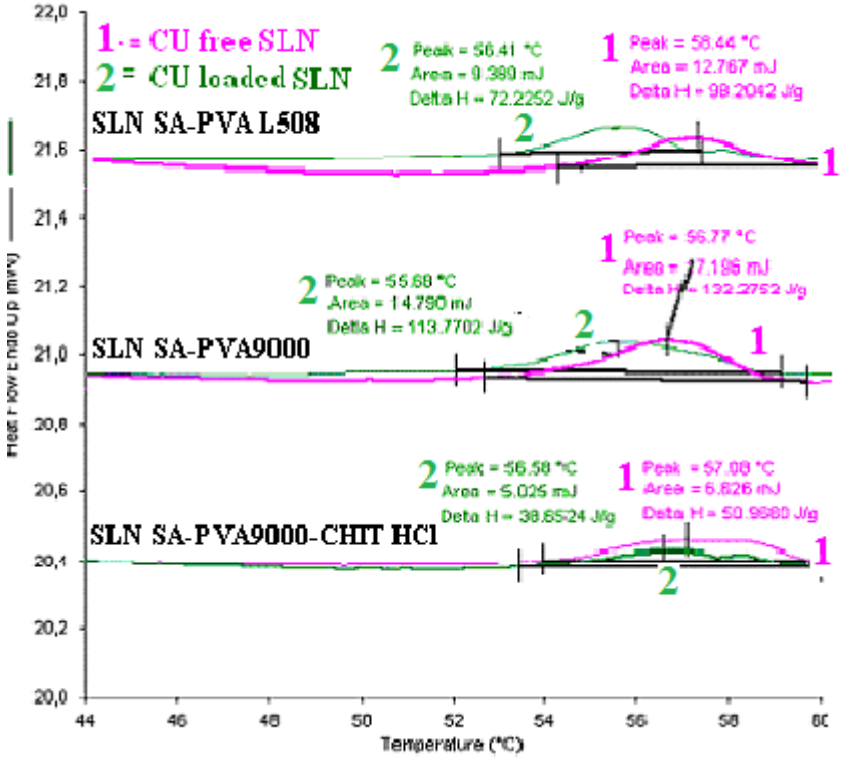

Figure 4 DSC thermograms of SA SLN in the presence and in the absence of CU.

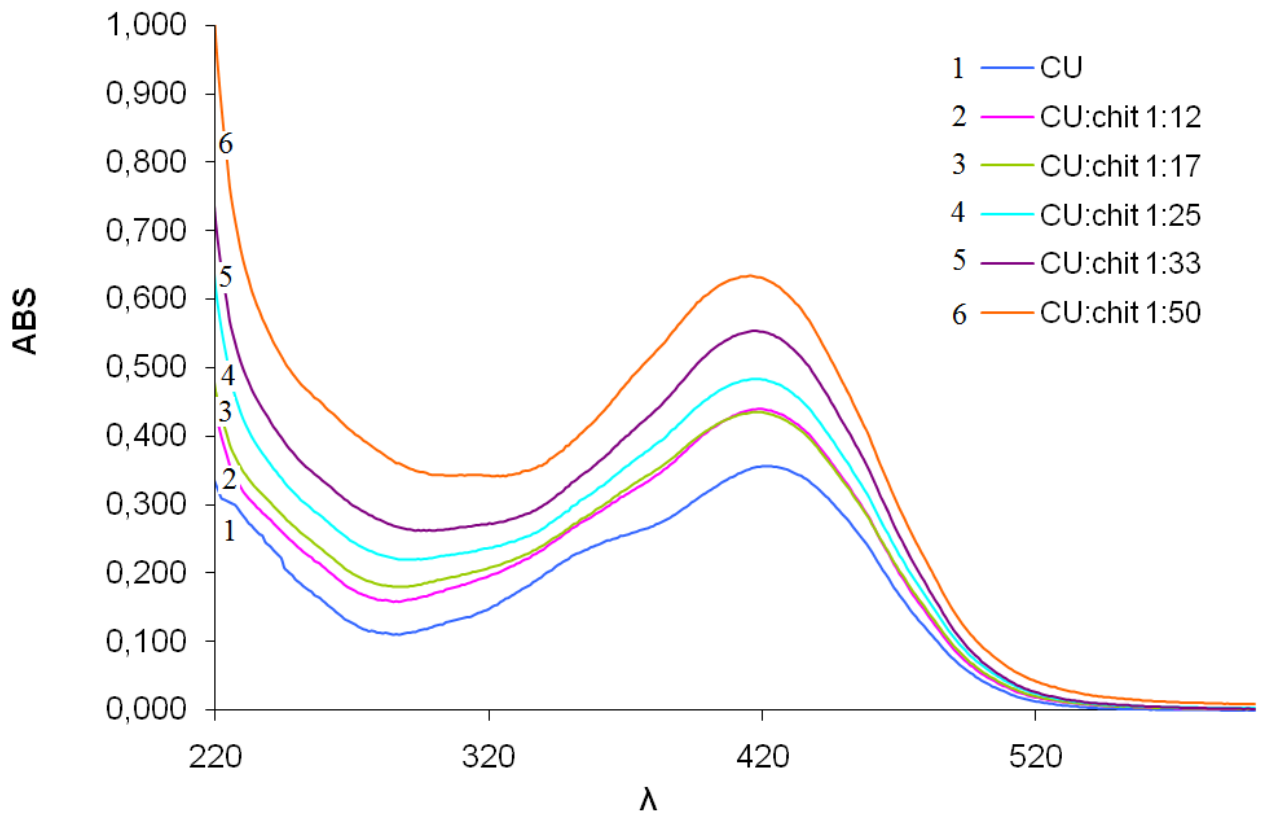

Figure 5 CU UV-VIS absorption spectra in the presence of different CU:chit w/w ratio.

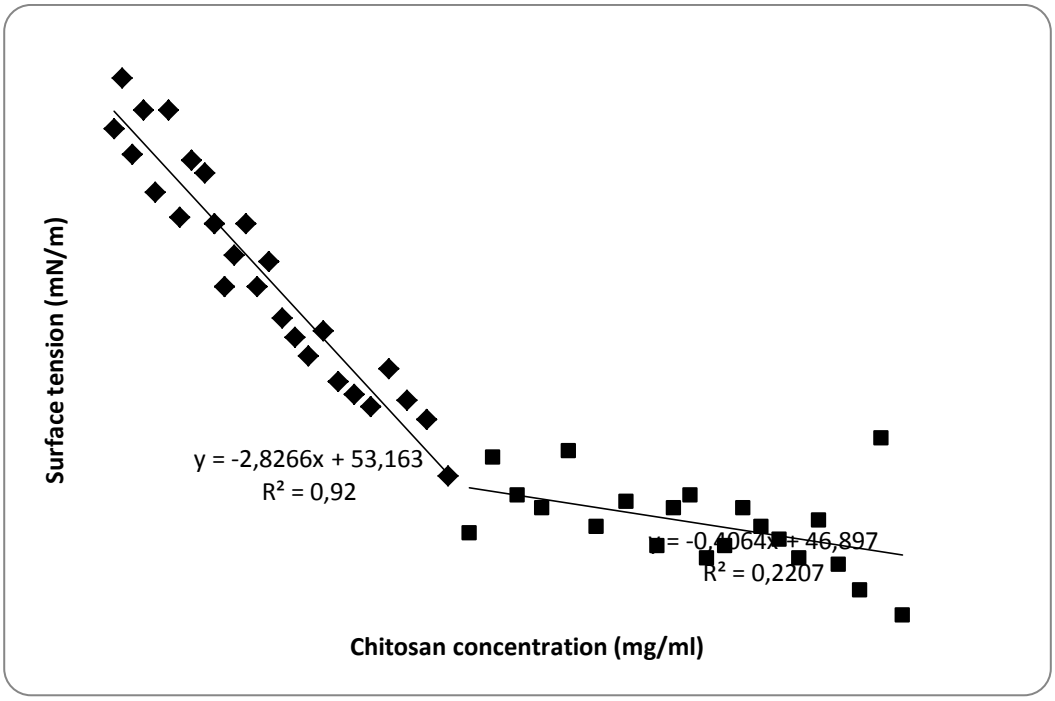

Figure 6 Chitosan surface tension determined in water.

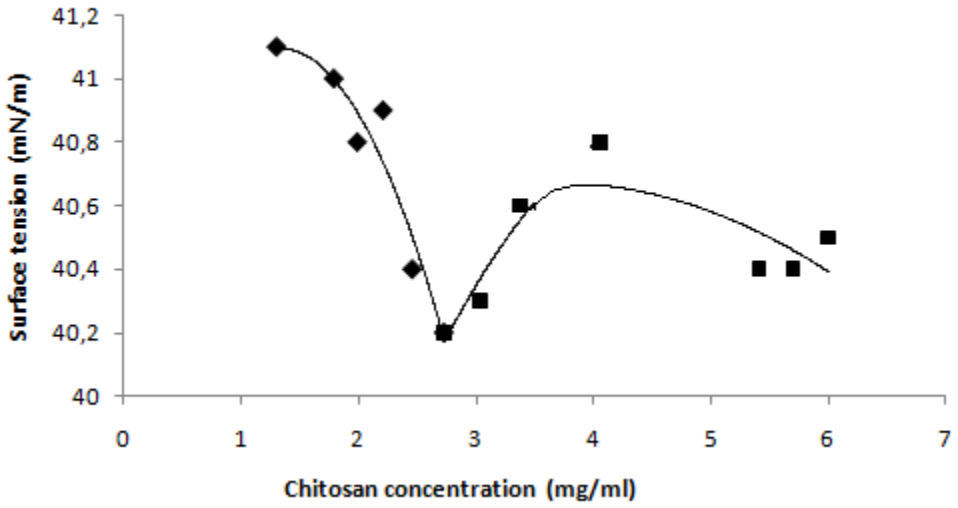

Figure 7 Chitosan surface tension determined in PVA 9000 aqueous solution.

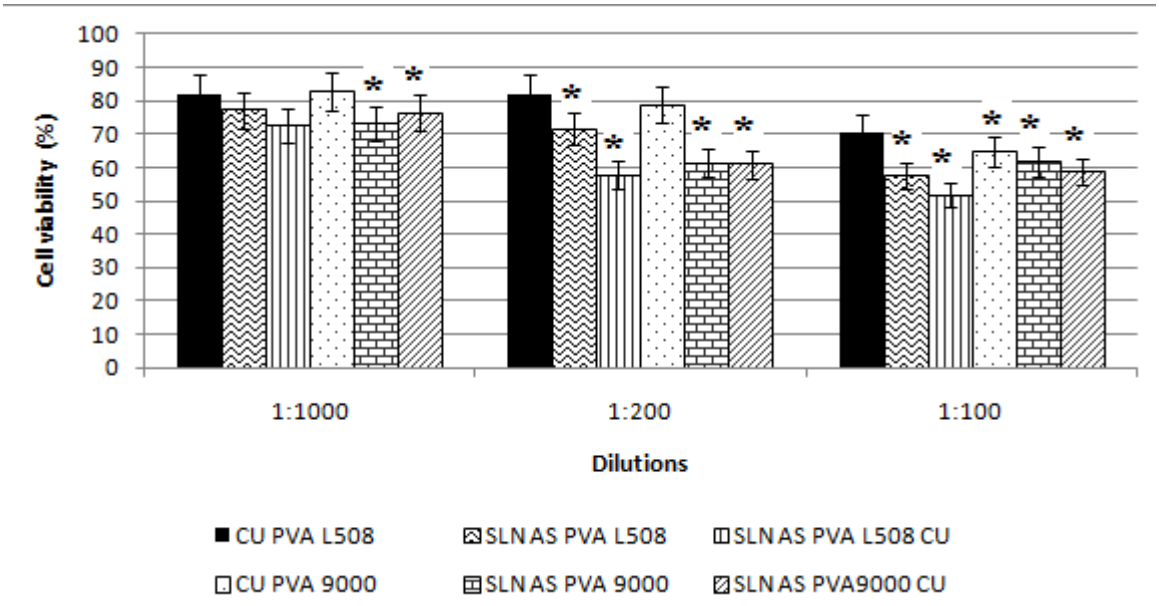

Figure 8 Cell viability of HCT-116 after 24 h exposure to the different CU-loaded and unloaded SLN at various dilution.

* $p<0.05$

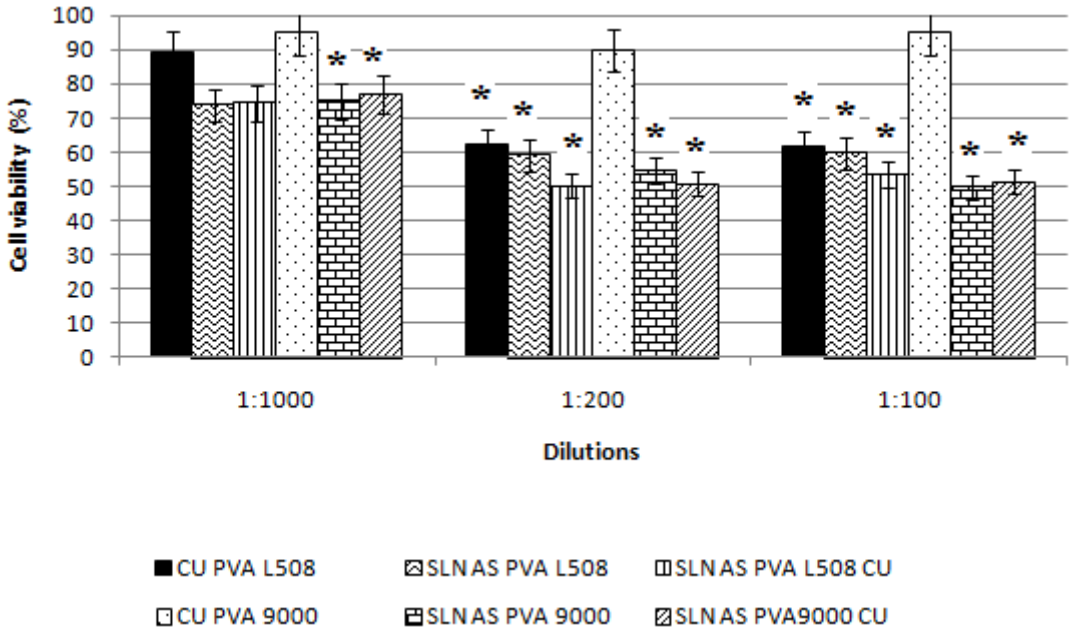

Figure 9 Cell viability of HCT-116 after 48 h exposure to the different CU-loaded and unloaded SLN at various dilution.

* $p<0.05$